

Analytic fit of the He-H<sub>2</sub> energy surface in the repulsive region

Arnold Russek

*Physics Department, The University of Connecticut, Storrs, Connecticut 06268*

Ramiro Garcia G.\*

*Instituto de Fisica, Universidad Nacional Autonoma de Mexico, Mexico 20, Distrito Federal*

(Received 4 January 1982)

Single-configuration Hartree-Fock calculations are reported on the HeH<sub>2</sub> triatomic-molecular system in the range of small He-H<sub>2</sub> separation,  $R$ , to complement earlier studies, so that the entire energy surface of interest to He on H<sub>2</sub> collisions in the low-keV collision-energy regime has now been determined. It is found that strong *repulsive* three-body polarization forces exist which dominate the physics of this collision-energy regime. Because a Legendre-polynomial expansion in the angular variable is found to be useless in this region of the energy surface, a new parametrization is introduced which includes both binary and three-body terms. The three-body terms are needed because the electron distribution in H<sub>2</sub> is different from the sum of the distributions of two individual H atoms.

## I. INTRODUCTION

Recent scattering experiments between rare-gas atoms and H<sub>2</sub> in the low-keV range of collision energies<sup>1-3</sup> have suggested the existence of strong, nonadditive valence forces deep in the repulsive region of the energy surface,<sup>3</sup> a surprising result since this region was thought to be dominated by screened Coulomb core-core type interactions, which give rise to additive forces. Indeed, the unmistakable conclusion from the experimental data was stated both tentatively and weakly in Ref. 3 for this very reason. Accordingly, it seemed worthwhile to investigate the repulsive part of the He-H<sub>2</sub> energy surface, the simplest of rare-gas H<sub>2</sub> systems and a prototype for the others, all of which behave in the same way in low-keV energy collisions.

A number of *ab initio* calculations on the He-H<sub>2</sub> triatomic-molecular system can be found in the literature<sup>4-11</sup> starting from 1963. There also exist two energy surface fittings to experimental data.<sup>12,13</sup> The existing literature is well summarized by Meyer *et al.*,<sup>11</sup> and none cover the full region required by keV energy collisions. In fact, the more recent and more accurate works have concentrated on the van der Waals minimum, which is located at He-H<sub>2</sub> separation  $R = 6.5a_0$ . This is approximately four times the separation  $r$  between the two protons in the H<sub>2</sub>, so that the van der Waals minimum is located in a region where the energy surface is nearly

isotropic in the angle  $\gamma$  between  $\vec{R}$  and  $\vec{r}$ . As a consequence, these works were able to parametrize the energy surface by expanding the angular dependence in Legendre polynomials

$$V(R, r, \gamma) = \sum_n V_n(R, r) P_n(\cos\gamma) \quad (1)$$

and retaining only the first two terms.

On the other hand, scattering experiments in the low-keV collision-energy range probe the energy surface deep in the repulsive region, where it is far more anisotropic and does not admit of a useful Legendre-polynomial expansion. Parenthetically, it may be remarked that the van der Waals minimum for He-H<sub>2</sub> has a well depth of only 1.0 meV. Such a shallow well is inconsequential for scattering experiments in the keV energy range, although experiments in this collision energy range are capable of "seeing" and exploring a more substantial well.

In this work *ab initio* calculations are presented for the deep repulsive region to complete the energy surface, and a new parametrization is developed to extend the Tang and Toennies theoretical model for the energy surface<sup>14</sup> to cover the entire energy surface. The Tang and Toennies model was originally introduced to describe the energy surface at intermediate and large distances ( $R \geq 4a_0$ ), which includes the region of the van der Waals minimum. For  $R \geq 4a_0$ , the first two terms of the Legendre-polynomial expansion are found to suffice; moreover, the coefficients of  $P_0$  and  $P_2$  can be taken as

functions of  $R$  only. Tang and Toennies further decomposed  $V_0$  and  $V_2$  into a self-consistent-field (SCF) contribution, a dispersion contribution, and a coupling correction:

$$V_n(R, r) = V_{n, \text{SCF}}(R) + V_{n, \text{disp}}(R) + V_{n, \text{corr}}(R). \quad (2)$$

The SCF contribution (a single-configuration Hartree-Fock calculation) yields a purely repulsive energy and is sufficient to describe the repulsive region of the energy surface at smaller values of  $R$ . In the limited range of  $R$ , which Tang and Toennies consider, they find that  $V_{0, \text{SCF}}$  and  $V_{2, \text{SCF}}$  can be accurately described by Born-Mayer potentials:  $A_n \exp(-b_n R)$ . The dispersion contribution, on the other hand, can only arise from a configuration interaction (CI) calculation; its existence altogether depends on electron-electron correlation. It is expressed as a series in inverse powers of  $R^2$ :

$$\sum_{i \geq 3} C_{n,i} / R^{2i}.$$

Finally, their correction term takes into account the effect of the repulsion on the dispersion.

In this work, the decomposition of the potential into  $V_{\text{SCF}}$ ,  $V_{\text{disp}}$ , and  $V_{\text{corr}}$  is retained, with  $V_{\text{disp}}$  and  $V_{\text{corr}}$  as given by Tang and Toennies.<sup>14</sup> Only  $V_{\text{SCF}}$  has to be modified to encompass the extended range of  $R$  here considered. *Ab initio* SCF calculations are here reported for values of  $R$  from 0 to  $3a_0$ , thus completing the range of  $R$  for which the energy surface has been calculated. In this small  $R$  region, neither the dispersion nor the coupling terms of the Tang and Toennies model make any appreciable contribution, so that only  $V_{\text{SCF}}$  need here be considered. It is found that a Legendre-polynomial expansion of  $V_{\text{SCF}}$  is inadequate in this small  $R$  region and that the dependence on the H-H separation,  $r$ , is quite important. Indeed, without the  $r$  dependence of the energy surface, the experimentally observed vibrational excitation could not take place. Calculations were therefore carried out for  $r = 1.2, 1.4, \text{ and } 1.6a_0$ . Moreover, a finer mesh of  $30^\circ$  increment was used for the angular dependence. A new parametrization for  $V_{\text{SCF}}$  is described in Sec. III, which adequately fits the calculated energy surface over a range of energy variation which spans more than four orders of magnitude. At the same time, this parametrization has the correct limiting forms at the singular points  $R_A = 0$  and  $R_B = 0$ , and the nonsingular, ordinary point  $R = 0$ . Finally, the individual terms in the new parametrization have physical significance and provide a better intuitive understanding of the energy surface.

## II. CALCULATIONS

SCF-LCAO-MO calculations (where LCAO and MO represent linear combination of atomic orbitals and molecular orbitals, respectively) have been made on the ground-state energy surface of the He-H<sub>2</sub> triatomic-molecular system using the IBMOL program and the SCF mode of the *GVB* program. The Gaussian basis set, taken from Brown and Hayes,<sup>15</sup> contained: (a) five  $s$ -type Gaussian functions contracted to four  $s$ -type atomic orbitals along with two  $p$ -type Gaussians centered on each H and (b) six  $s$ -type Gaussians contracted to four atomic orbitals along with two  $p$ -type Gaussians centered on the He. This basis set adequately describes polarization contributions to the energy surface.

As a single-configuration calculation, it can give only the  $V_{\text{SCF}}$  contribution of the Tang and Toennies model. Consequently, there was no point to extending the calculations beyond  $R = 3$ , which is well into the asymptotic region of  $V_{\text{SCF}}$  and provides sufficient overlap for comparison with the accurate results of Meyer *et al.*<sup>11</sup> It can be seen from Table I that at  $R = 2$  and 3, their SCF energies differ from the present results by approximately 0.002 hartree (1 hartree = 27.2 eV). Moreover, at the two comparison values of  $R$ , the best multiconfiguration results of Meyer *et al.* are lower than the SCF results by an amount less than 0.007 hartree, thereby validating the use of SCF calculations for representing the repulsive region of the energy surface. The accuracy of the present calculations, including correlation corrections from a CI calculation, are, therefore, or the order of 0.01 hartree. For this reason,

TABLE I. Comparison with the results of Meyer *et al.*

$\gamma$	$R$	$r$	$E_{\text{int}}$			
			Present	Meyer <i>et al.</i> <sup>a</sup>	SCF Meyer <i>et al.</i> <sup>a</sup> CI	
0°	2	1.2	0.195	0.195	0.188	
		1.4	0.215	0.211	0.205	
		1.6	0.232	0.230	0.226	
	3	1.2	0.030	0.031	0.029	
		1.4	0.036	0.036	0.033	
		1.6	0.042	0.041	0.038	
	90°	2	1.2	0.152	0.153	0.145
			1.4	0.154	0.154	0.146
			1.6	0.155	0.154	0.145
3		1.2	0.024	0.025	0.022	
		1.4	0.026	0.026	0.023	
		1.6	0.029	0.028	0.024	

<sup>a</sup>Reference 11.

TABLE II. He-H<sub>2</sub> interaction energy. Interaction energy as a function of  $R$ ,  $r$ , and  $\gamma$ . Columns labeled  $E_{\text{int}}$  give the *ab initio* calculations. Columns labeled  $V_{\text{par}}$  give the results of the parametric fit, Eq. (7), with  $Z_{\text{H}}Z_{\text{He}}=2$ ,  $\lambda_c=3.20$ ,  $A_2=1.2$ ,  $\lambda_p=1.742$ ,  $A_3=2.76$ ,  $B=2.18$ , and  $b=2.20$ .

$R$	$r$	$\gamma=0^\circ$		$\gamma=30^\circ$		$\gamma=60^\circ$		$\gamma=90^\circ$	
		$E_{\text{int}}$	$V_{\text{par}}$	$E_{\text{int}}$	$V_{\text{par}}$	$E_{\text{int}}$	$V_{\text{par}}$	$E_{\text{int}}$	$V_{\text{par}}$
0	1.2	2.41	2.40	2.41	2.40	2.41	2.40	2.41	2.40
	1.4	1.88	1.89	1.88	1.89	1.88	1.89	1.88	1.89
	1.6	1.53	1.56	1.53	1.56	1.53	1.56	1.53	1.56
0.5	1.2	16.70	16.19	4.00	3.93	1.81	1.81	1.58	1.46
	1.4	6.87	6.73	2.90	2.96	1.44	1.53	1.36	1.26
	1.6	3.76	3.84	2.06	2.23	1.24	1.30	1.18	1.10
1.0	1.2	2.35	2.31	1.36	1.36	0.84	0.77	0.78	0.64
	1.4	3.64	3.57	1.47	1.50	0.78	0.73	0.73	0.59
	1.6	6.59	6.42	1.51	1.59	0.70	0.69	0.68	0.55
1.5	1.2	0.52	0.53	0.45	0.43	0.37	0.32	0.36	0.28
	1.4	0.60	0.64	0.47	0.47	0.37	0.32	0.35	0.27
	1.6	0.74	0.80	0.49	0.52	0.35	0.31	0.34	0.26
2.0	1.2	0.20	0.19	0.18	0.17	0.16	0.14	0.15	0.12
	1.4	0.22	0.22	0.19	0.18	0.16	0.14	0.15	0.12
	1.6	0.23	0.25	0.20	0.20	0.17	0.14	0.16	0.12
3.0	1.2	0.030	0.033	0.029	0.030	0.025	0.026	0.024	0.024
	1.4	0.036	0.036	0.033	0.032	0.028	0.026	0.026	0.023
	1.6	0.042	0.040	0.038	0.034	0.032	0.026	0.029	0.023

the results presented in Table II are given only to two decimal places, except at  $R=3$ , where they are given to two significant figures.

With the geometry shown in Fig. 1, the energy

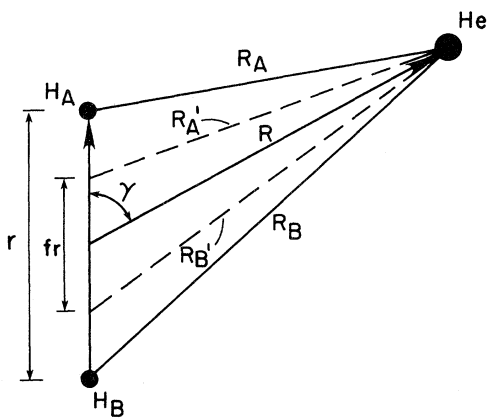


FIG. 1. Molecular geometry. Independent coordinates are  $R$ ,  $r$ , and  $\gamma$ . Distances between the He nucleus and the two H nuclei are denoted by  $R_A$  and  $R_B$ . Distances  $R'_A$  and  $R'_B$  are defined in Eqs. (9).

surface is given for 63 coordinate sets,  $R$ ,  $r$ ,  $\gamma$ , in the columns labeled  $E_{\text{int}}$  of Table II, where

$$E_{\text{int}} = V_{\text{SCF}} - E_{\text{He}} - E_{\text{H}_2}(r). \quad (3)$$

Hence, for any value of  $r$ ,  $E_{\text{int}}$  is the interaction energy between a He atom and an H<sub>2</sub> molecule with proton-proton separation  $r$ . Physically, it represents the scattering potential for a slow (low-keV) He atom impinging on a ground-state H<sub>2</sub> molecule with fixed separation  $r$  during the interaction time. For all practical purposes, such is the case for small angle scattering in the low-kV energy regime. On the one hand, the collision is slow enough so that the adiabatic electronic energy acts as an effective potential for the nuclear motion. On the other hand, the collision time, of the order of  $10^{-16}$  sec, is short compared with vibrational periods ( $\sim 10^{-14}$  sec) and rotational periods ( $\sim 10^{-12}$  sec), so that  $\vec{r}$  effectively remains constant in both magnitude and direction during the collision. For convenience in converting from  $E_{\text{int}}$  to  $V_{\text{SCF}}$  at the three values of  $r$  here considered:

$$E_{\text{int}} = V_{\text{SCF}} + \begin{cases} 3.984 \text{ hartree at } r = 1.2a_0, \\ 3.994 \text{ hartree at } r = 1.4a_0, \\ 3.988 \text{ hartree at } r = 1.6a_0. \end{cases} \quad (4)$$

### III. ENERGY SURFACE

#### A. Atom-atom potential

For heuristic purposes, the two-body atom-atom energy will be considered first, because an understanding of this interaction is essential to the understanding of the atom-molecule energy. At small internuclear separations, where the Coulomb repulsion between the nuclei dominates, the interaction energy should be a screened Coulomb type, essentially a Bohr potential. This arises from point nuclei, each partially screened by a rigidly fixed electron cloud held so firmly in place by the respective parent nucleus that it is negligibly distorted by the other atom. At longer ranges, the interaction energy goes over to a Born-Mayer type, which somehow takes into account the Pauli contribution to the energy as the two electron clouds overlap, thus making it a polarization contribution to the energy. At still larger internuclear separations, the van der Waals attraction, which is also a polarization contribution, dominates. That term will, however, be omitted from the present discussion, so that the atom-atom potential is of the form

$$V_{\text{atom-atom}} = \frac{Z_1 Z_2}{R_{12}} e^{-\lambda_c R_{12}} + A e^{-\lambda_p R_{12}}. \quad (5)$$

where  $R_{12}$  is the internuclear separation. From the above discussion, it is reasonable to expect that  $\lambda_c$  should be larger than  $\lambda_p$  so that the screened Coulomb core interaction is shorter range than the Born-Mayer polarization interaction. The potential form given by Eq. (5) is indeed found to describe the He-H interaction, with the relative sizes of the respective ranges conforming to expectation.

#### B. Atom-molecule potential

Purely additive two-body forces would yield for the He-H<sub>2</sub> atom-molecule interaction:

$$V_{\text{two-body}} = Z_{\text{H}} Z_{\text{He}} \left[ \frac{e^{-\lambda_c R_A}}{R_A} + \frac{e^{-\lambda_c R_B}}{R_B} \right] + A (e^{-\lambda_p R_A} + e^{-\lambda_p R_B}),$$

where  $R_A$  and  $R_B$  are the distances from the He nucleus to the respective protons. This cannot, however, be the full interaction. The second term on the right-hand side of Eq. (5) has been characterized as a polarization term, due to the overlap of electron wave functions and the Pauli exclusion principle. Being a polarization term, it should therefore alter when two hydrogen atoms combine to form a molecule, since the H<sub>2</sub> molecule has an excess electron distribution between the two protons drawn at the expense of the electron distributions centered on each proton. Consequently, one would expect the strength,  $A$ , of the two-body polarization term for the He-H<sub>2</sub> system to be reduced from that which was found for the He-H atom-atom system. This reduction should be compensated by the appearance of an additional term of the form  $A' \exp(-\lambda_p R)$  to take into account the electron distribution of the H<sub>2</sub> which is centered midway between the two protons, i.e., at  $R=0$ . One additional correction must be made. The point  $R=0$  has no potential singularity; it is a perfectly ordinary point in the eigenvalue equation for the electronic wave function. Therefore, it cannot have a discontinuous slope at  $R=0$ , so that the  $R$ -dependent polarization should be of the form

$$A_3 e^{-\lambda_p R} - B e^{-bR} \quad (6a)$$

with

$$A_3 \lambda_p = B b \quad (6b)$$

in order to ensure continuous derivative at  $R=0$ . Thus, the parametric form suggested here for the SCF contribution to the interaction energy is

$$V_{\text{SCF}} = Z_{\text{H}} Z_{\text{He}} \left[ \frac{e^{-\lambda_c R_A}}{R_A} + \frac{e^{-\lambda_c R_B}}{R_B} \right] + A_2 (e^{-\lambda_p R_A} + e^{-\lambda_p R_B}) + A_3 e^{-\lambda_p R} - B e^{-bR}, \quad (7)$$

where  $A_2$  describes the strength of the additive two-body contribution to the polarization interaction, while  $A_3$  describes the three-body correction term, with  $B$  and  $b$  characterizing the saturation of that term in the vicinity of  $R=0$ . Table II and Fig. 2 show the best fit of the parametric form (7) for  $V_{\text{SCF}}$  with the *ab initio* calculations, obtained with  $Z_{\text{H}} Z_{\text{He}} = 2$ ,  $\lambda_c = 3.20$ ,  $A_2 = 1.2$ ,  $\lambda_p = 1.742$ ,  $A_3 = 2.76$ ,  $B = 2.18$ , and  $b = 2.2$ , all quantities being given in atomic units.

It can be seen from Fig. 2 that the parametric

form (7) describes the energy surface for small values of  $R$  quite well. That is to be expected since the small- $R$  region is dominated by the core-core repulsions and is insensitive to minor details of the electron distribution. On the other hand, the fit at larger values of  $R$ , although adequate to describe most collisions in the keV energy range, is not up to the standards demanded by chemists, who must deal with very low-energy collisions. They require better accuracy in the large- $R$  region ( $R \geq 2$  a.u.), where the parametric form (7) consistently overstates the angular dependence of the energy surface. The fault lies not with the general concept of the model here proposed, but rather with the specific form suggested in Eq. (7). There, the excess electron distribution between the two protons has, for simplicity, been taken into account by a spherically symmetric distribution centered at  $R=0$ . As Fig. 2 shows, even this rough approximation goes a long way toward describing the energy surface. However, an even better approximation of the distorted electron distribution in  $H_2$  can be obtained by centering the electron distribution for each H not on the nucleus itself, but at some point between the two protons in addition to the distribution centered at  $R=0$ . With the centers of the displaced distributions at  $\pm fr/2$ , the improved parametric form is given by

$$V_{SCF} = Z_H Z_{He} \left[ \frac{e^{-\lambda_c R_A}}{R_A} + \frac{e^{-\lambda_c R_B}}{R_B} \right] + A (e^{-\lambda_p R'_A} + e^{-\lambda_p R'_B}) + A_3 e^{-\lambda_p R} - B e^{-bR}, \quad (8)$$

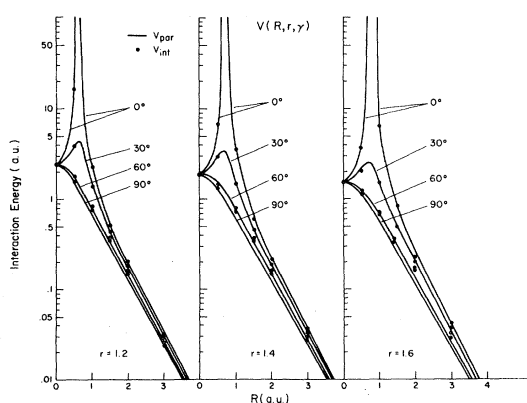


FIG. 2. He- $H_2$  interaction energy. Results of the *ab initio* calculations are taken from the columns labeled  $E_{int}$  of Table II, and are shown as the solid black circles. Curves show the fit obtained with the parametric form Eq. (7) with the parameters listed in Table II.

where

$$R'_A = [R^2 + (fr/2)^2 - frR \cos\gamma]^{1/2}, \quad (9a)$$

$$R'_B = [R^2 + (fr/2)^2 + frR \cos\gamma]^{1/2}. \quad (9b)$$

It should be noted that the Bohr term, which describes the contributions of the nuclei plus that part of the electronic distribution rigidly held by each nucleus, is still a function of  $R_A$  and  $R_B$ . Only the polarization terms have centers shifted to lie between the two nuclei. The subscript 2 on the strength of this potential has been dropped, since it is no longer a two-body contribution. Figure 3 and Table III show the fit obtained with the parametric form given by Eq. (8) with the parameters listed in Table III. The interaction energies which follow from Eq. (8) are presented in the columns labeled  $V_{par2}$ . For comparison, the values from Table II, which follow from Eq. (7), are listed in the columns marked  $V_{par1}$ . The *ab initio* calculations from Table II are also listed. The potential form given by Eq. (8) gives a poorer representation of the energy surface in the small- $R$  region than does Eq. (7), and for good reason. When the He nucleus penetrates into the  $H_2$  interior, the  $H_2$  electron distribution will further distort, with at least some of the excess distribution between the two protons being forced out. To avoid the complexity of parameters which are  $R$  dependent in this work, the small- $R$  region has been omitted from consideration in Fig. 3 and Table III.

Although the second term of Eq. (8) is continuous, it has unphysical discontinuities in derivative at the ordinary points  $R'_A=0$  and  $R'_B=0$ . A realistic potential, generated by a nonsingular electron

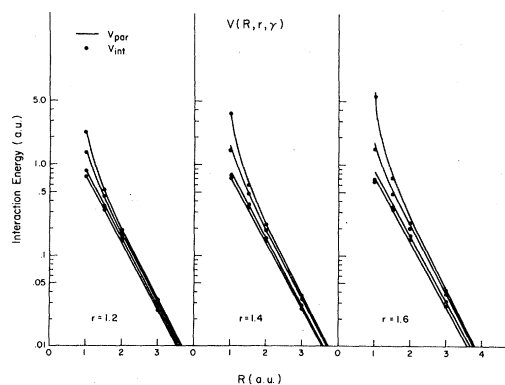


FIG. 3. He- $H_2$  interaction energy. Results of the *ab initio* calculations are taken from the columns labeled  $E_{int}$  of Table II. For convenience, these results are repeated in the columns labeled  $E_{int}$  in Table III. *Ab initio* calculations are shown as the solid black circles. Curves show the best fit obtained with the parametric form Eq. (8) with the parameters listed in Table III.

TABLE III. He-H<sub>2</sub> interaction energy. Interaction energy as a function of  $R$ ,  $r$ , and  $\gamma$ . Columns labeled  $E_{\text{int}}$  give the *ab initio* calculations. Columns labeled  $V_{\text{par2}}$  give the results of the parametric fit, Eq. (8), with  $Z_{\text{H}}Z_{\text{He}}=2$ ,  $\lambda_p=1.742$ , and  $b=2.20$ . Remaining parameters are  $r$  dependent. For  $r=1.2$ ,  $f=0.7$ ,  $A=1.70$ ,  $A_3=1.73$ , and  $B=1.37$ ; for  $r=1.4$ ,  $f=0.8$ ,  $A=1.50$ ,  $A_3=2.51$ , and  $B=1.99$ ; for  $r=1.6$ ,  $f=0.85$ ,  $A=1.30$ ,  $A_3=3.74$ , and  $B=2.96$ . Columns labeled  $V_{\text{par1}}$  are repeated from Table II for ease of comparison.

$R$	$r$	$E_{\text{int}}$	$\gamma=0^\circ$		$E_{\text{int}}$	$\gamma=30^\circ$		$E_{\text{int}}$	$\gamma=60^\circ$		$E_{\text{int}}$	$\gamma=90^\circ$	
			$V_{\text{par1}}$ Eq. (7)	$V_{\text{par2}}$ Eq. (8)		$V_{\text{par1}}$ Eq. (7)	$V_{\text{par2}}$ Eq. (8)		$V_{\text{par1}}$ Eq. (7)	$V_{\text{par2}}$ Eq. (8)		$V_{\text{par1}}$ Eq. (7)	$V_{\text{par2}}$ Eq. (8)
1.0	1.2	2.35	2.31	2.31	1.36	1.36	1.42	0.84	0.77	0.87	0.78	0.64	0.75
	1.4	3.64	3.57	3.57	1.47	1.50	1.58	0.78	0.73	0.83	0.73	0.59	0.69
	1.6	6.59	6.42	6.42	1.51	1.59	1.71	0.70	0.69	0.83	0.68	0.55	0.70
1.5	1.2	0.52	0.53	0.52	0.45	0.43	0.44	0.37	0.32	0.35	0.36	0.28	0.32
	1.4	0.60	0.64	0.64	0.47	0.47	0.49	0.37	0.32	0.35	0.35	0.27	0.31
	1.6	0.74	0.80	0.81	0.49	0.52	0.56	0.35	0.31	0.37	0.34	0.26	0.32
2.0	1.2	0.20	0.19	0.19	0.18	0.17	0.17	0.16	0.14	0.15	0.15	0.12	0.14
	1.4	0.22	0.22	0.22	0.19	0.18	0.19	0.16	0.14	0.15	0.15	0.12	0.14
	1.6	0.23	0.25	0.26	0.20	0.20	0.22	0.17	0.14	0.16	0.16	0.12	0.15
3.0	1.2	0.030	0.033	0.031	0.029	0.030	0.029	0.025	0.026	0.026	0.024	0.024	0.025
	1.4	0.036	0.036	0.036	0.033	0.032	0.033	0.028	0.026	0.028	0.026	0.023	0.026
	1.6	0.042	0.040	0.042	0.038	0.034	0.038	0.032	0.026	0.031	0.029	0.023	0.028

distribution would be perfectly regular at these points. It is not difficult to modify the potential to make the derivative continuous, as was done for the  $R$ -dependent potential. However, since this potential is not being considered in the vicinity of  $R'_A$  or  $R'_B$  equal to zero, no attempt was made to do so. It should be made clear that the term "potential" has, for heuristic reasons, been used rather loosely in the above discussion. It is certainly not an electrostatic potential energy arising from a charge distribution. Rather, it is a term in the adiabatic electronic energy and includes kinetic energy of the electrons as well as electrostatic potential energy. Nevertheless, despite the fact that the adiabatic electronic energy is more complicated, any symmetry in the electronic wave functions will show up as a symmetry in the energy surface and the energy surface must be regular at any point in space where no singularity exists. That is really all that was said.

Finally, attention should be drawn to a peculiar feature of the energy surface in the vicinity of  $\gamma=90^\circ$ . With the He nucleus along the perpendicular bisector to the H<sub>2</sub> axis, a repulsive potential, in addition to pushing the He and H<sub>2</sub> away from each other, would also be expected to push the two H atoms apart. Thus,  $E_{\text{int}}$  should decrease as  $r$  increases; the gradient of the energy surface with respect to  $r$  should be negative. The *ab initio* calculations for  $E_{\text{int}}$  in Table II indeed show the expected

behavior at small values of  $R$  for  $R$  less than  $2.0a_0$ . However, at about  $2.0a_0$ , a crossover occurs and for larger values of  $R$ , the gradient with respect to  $r$  is positive. In this large- $R$  region, the helium atom, while pushing the entire H<sub>2</sub> system away from it ( $\partial E_{\text{int}}/\partial R$  is negative for all  $R$ ), is actually drawing the two H atoms closer to each other. It can be seen in Table III that the improved parametrization,  $V_{\text{par2}}$ , exhibits the proper behavior at  $\gamma=90^\circ$ , whereas  $V_{\text{par1}}$  does not. It is also evident that for  $\gamma=0$ ,  $\partial E_{\text{int}}/\partial r$  is always positive. Such behavior is, however, expected even from purely repulsive potentials. The He repels the closer H with a larger force than the one further away, thus pushing the two H atoms toward each other. It is therefore not surprising that both parametrizations exhibit the proper behavior at  $\gamma=0^\circ$ . At intermediate angles, the situation is ambiguous, so that no qualitative conclusions can be drawn. Only at  $90^\circ$  is the difference in behavior clear cut. The qualitative agreement of  $V_{\text{par2}}$  with the *ab initio* calculations may not be taken as a strong verification of the parametric form given by Eq. (8), since  $r$ -dependent parameters are used in the fit. The main thrust of the argument is that the behavior of the energy surface at large  $R$  calls for  $r$ -dependent parameters. There is, moreover, good physical justification for having the parameters in the polarization terms dependent on  $r$ , since the amount and distribution

of the excess central distribution of the electrons in the  $H_2$  molecule does, in fact, depend on  $r$ .

#### ACKNOWLEDGMENTS

One of the authors (R.G.G.) wishes to express his gratitude to the University of Connecticut for its

hospitality during his sabbatic leave from the Physics Institute of the University of Mexico and to acknowledge support from CONACyT Grant No. PCCBNAL-790086. The other author (A.R.) acknowledges support from NSF Grant No. INT 80-17035.

---

\*On sabbatic leave at the University of Connecticut.

<sup>1</sup>A. V. Bray, D. S. Newman, and E. Pollack, Phys. Rev. A **15**, 2261 (1977).

<sup>2</sup>N. Andersen, M. Vedder, A. Russek, and E. Pollack, J. Phys. B **11**, L493 (1978).

<sup>3</sup>N. Andersen, M. Vedder, A. Russek, and E. Pollack, Phys. Rev. A **21**, 782 (1980).

<sup>4</sup>C. S. Roberts, Phys. Rev. **131**, 203 (1963).

<sup>5</sup>M. Krauss and F. H. Mies, J. Chem. Phys. **42**, 2703 (1965).

<sup>6</sup>M. D. Gordon and D. Secrest, J. Chem. Phys. **52**, 120 (1970).

<sup>7</sup>B. Tsapline and W. Kutzelnigg, Chem. Phys. Lett. **23**, 173 (1973).

<sup>8</sup>W. Meyer, Chem. Phys. **17**, 27 (1976).

<sup>9</sup>A. W. Raczkowski and W. A. Lester, Jr., Chem. Phys. Lett. **47**, 45 (1977).

<sup>10</sup>A. J. Takhar, Chem. Phys. Lett. **46**, 453 (1977).

<sup>11</sup>W. Meyer, P. C. Hariharan, and W. Kutzelnigg, J. Chem. Phys. **73**, 1880 (1980).

<sup>12</sup>R. Gegenbach and Ch. Hahn, Phys. Lett. **15**, 604 (1972).

<sup>13</sup>R. Shaefer and R. G. Gordon, J. Chem. Phys. **58**, 5422 (1973).

<sup>14</sup>K. T. Tang and J. P. Toennies, J. Chem. Phys. **68**, 5501 (1978).

<sup>15</sup>P. J. Brown and E. F. Hayes, J. Chem. Phys. **55**, 922 (1971).